Available online at www.sciencedirect.com
ScienceDirect
Journal of Nuclear Materials 372 (2008) 32–35
journal of nuclear materials
www.elsevier.com/locate/jnucmat

Simulations of H_2O_2 concentration profiles in the water surrounding spent nuclear fuel

Fredrik Nielsen, Karin Lundahl, Mats Jonsson *

KTH Chemical Science and Engineering, Nuclear Chemistry, Royal Institute of Technology, SE-100 44, Sweden

Received 15 September 2006; accepted 30 January 2007

Abstract

A simple mathematical model describing the hydrogen peroxide concentration profile in water surrounding a spent nuclear fuel pellet as a function of time has been developed. The water volume is divided into smaller elements, and the processes that affect hydrogen peroxide concentration are applied to each volume element. The model includes production of H_2O_2 from α-radiolysis, surface reaction between H_2O_2 and UO_2 and diffusion. Simulations show that the surface concentration of H_2O_2 increases fairly rapidly and approaches the steady-state concentration. The time to reach steady-state is sufficiently short to be neglected compared to the times of interest when simulating spent fuel dissolution under deep repository conditions. Consequently, the steady-state approach can be used to estimate the rate for radiation-induced spent nuclear fuel dissolution.

1. Introduction

The solubility of UO_2 is assumed to limit the release of radio-toxic species from a future deep repository for spent nuclear fuel to the environment [1]. Under reducing conditions, i.e., the expected conditions at the depth of a deep repository, the solubility of UO_2 in ground water is very low and the release rate is therefore also expected to be low [2]. Radiation from the spent nuclear fuel in contact with water will cause radiolysis of water, producing reactive radical and molecular products. Both oxidants ($OH^{\bullet}$, H_2O_2, $O_2^{\bullet-}$, $HO_2^{\bullet}$ and O_2) and reductants (e_{aq}^-, $H^{\bullet}$ and H_2) are produced upon radiolysis of water [3]. For kinetic reasons, the oxidants produced alter the otherwise reducing conditions, and can thereby cause oxidation and dissolution of the spent nuclear fuel matrix. When carbonate is present, as in Swedish ground water where the concentration is 2–10 mM [4], $OH^{\bullet}$ will be quantitatively converted into $CO_3^{\bullet-}$, this also being a strong oxidant ($E^0 = 1.9$ V and 1.59 V vs. NHE, respectively [5,6]). Carbonate is also known to form strong soluble complexes with UO_2^{2+} [7] and thereby enhance the solubility of U(VI).

The kinetics for reactions between different oxidants and the spent fuel matrix (UO_2) have been studied quite extensively [8,9]. On the basis of these results it has been possible to assess the relative reactivity of the radiolytically formed oxidants [10]. The relative importance, or impact, of the different radiolysis products has been discussed for several years. However, it should be stressed that the relative reactivity is not the same as the relative importance of the reactant. The latter being the product of the reactivity (rate constant) and the concentration of the reactant. Very recently, it was shown that the molecular products, although in general being less reactive than some of the oxidizing radicals, have the highest impact (relative importance) for all types of radiation (except for very short irradiation time where the impact of radicals is significant). The rationale for this is simply that the concentration of molecular products is many orders of magnitude higher than the concentration of radical products. In an aqueous UO_2 system exposed to α-radiation, the relative impact of H_2O_2 was found to be 99.9–100% [10]. Hence, the only

* Corresponding author. Fax: +46 8790 8772.
E-mail address: matsj@nuchem.kth.se (M. Jonsson).

0022-3115/$ - see front matter © 2007 Elsevier B.V. All rights reserved.
doi:10.1016/j.jnucmat.2007.01.279

oxidant that must be accounted for in a safety assessment of a future deep repository is H_2O_2. At HCO_3^- concentrations higher than 1 mM the rate limiting step in the reaction between H_2O_2 and UO_2 has been shown to be oxidation while at lower concentrations dissolution of oxidized UO_2 influences the kinetics [9]. Consequently, the rate of spent fuel dissolution will be equal to the rate of H_2O_2 consumption. Since the rate constant for this process is well known, the only missing parameter is the concentration of H_2O_2. This will be strongly connected to the dose rate which in turn depends on the fuel age and burn-up. We have recently developed a model describing the geometrical α- and β-dose distribution as function of fuel age and burn-up [11]. Indeed, the maximum rate of fuel dissolution can never exceed the rate of H_2O_2 production in the system. However, the question is how long it takes before steady-state is reached? To shed some light on this and to provide means for simplified, yet accurate, simulations of spent nuclear fuel dissolution, we have simulated the H_2O_2 concentration profile evolution with time taking into account the radiolytic production of H_2O_2, diffusion of H_2O_2 and consumption of H_2O_2 by reaction with a UO_2 surface.

2. Methods

The concept of the model underlying the simulations is fairly simple. The system was modeled in one dimension starting at the fuel surface. The volume is divided into smaller elements, and the H_2O_2 concentration for each volume element is stored in a vector. For each time-step the H_2O_2 concentration in each element is calculated taking the following processes into account:

1. Radiolytic production of H_2O_2.
2. Diffusion due to concentration gradients.
3. Reaction between H_2O_2 and UO_2 (only the first volume element).

The radiolytic production of H_2O_2 was determined by using the geometrical α-dose distribution determined from the model mentioned above. The dose rate used in the majority of the simulations is for spent fuel at 100 years, with a burn-up of 38 MWd/kg [11]. The geometrical α-dose distribution provides the dose rate as a function of distance which must be converted into the rate of H_2O_2 production as a function of distance from the surface. The simplest approach for this would have been to use the radiation chemical yield, i.e., the *G*-value, directly. However, to make sure that the rate of production does not depend on H_2O_2 concentration we performed numerical simulations employing MAKSIMA-CHEMIST [12]. On the basis of these simulations and the geometrical dose distribution a polynomial describing the rate of H_2O_2 production (r/mol dm^{-3} s^{-1}) as a function of distance (x/μm) was derived (Eq. (1)):

$$r_{H_2O_2} = ax^3 + bx^2 + cx + d. \quad (1)$$

For spent fuel at 100 years, the constants are:

$$a = -1.58 \times 10^{-12},$$
$$b = 1.46 \times 10^{-10},$$
$$c = -4.77 \times 10^{-9},$$
$$d = 5.67 \times 10^{-8}.$$

It should be noted that the MAKSIMA-CHEMIST simulations gave virtually the same result as expected from using the *G*-value. The surface reaction is accounted for in the first volume element using the rate expression previously derived (Eq. (2)) [10]:

$$r_{ox} = k_{ox}[H_2O_2]. \quad (2)$$

The rate constant for the reaction between H_2O_2 and UO_2, k_{ox}, has been determined experimentally to 7.333×10^{-8} m s^{-1} [9]. Since spent nuclear fuel also contains metallic ε-particles potentially capable of catalyzing H_2O_2 decomposition and reaction between H_2O_2 and H_2 without leading to UO_2 oxidation, the rate constant for the H_2O_2 consumption was varied in the simulations in order to study the impact of such reactions. A higher rate constant for consumption of H_2O_2 results in a lower steady-state concentration and thereby a lower rate of spent fuel dissolution.

Diffusion between the volume elements is determined by the concentration gradient between two adjacent elements using Fick's first law (Eq. (3)):

$$J = -D\frac{dc}{dx}. \quad (3)$$

The diffusion coefficient used for H_2O_2 was 1×10^{-9} m^2 s^{-1}.

The contributions from the above processes are added together and applied to the concentration vector to determine a new concentration vector for each time-step. To simulate the time evolution of the concentration profile an iterative process based on MATLAB was used. The time-step, dt, and distance step, dx, were chosen in order to achieve results with high resolution without slowing down the calculations. The time-step used was 0.5 ms, and the distance step was 1 μm. Apart from varying the rate constant for the surface reaction we also varied the volume, i.e., the total distance from the surface.

3. Results and discussion

In Fig. 1 the concentration profile for $k = 7.333 \times 10^{-5}$ m s^{-1} is given at 1, 3, 10 and 41 s. For comparison, the steady-state concentration for the system is also given in the figure. The steady-state concentration is calculated using Eq. (4):

$$[H_2O_2]_{s\text{-}s} = \frac{\overline{r_{H_2O_2}}}{k_{ox}}\delta_{max}, \quad (4)$$

where $[H_2O_2]_{s\text{-}s}$ denotes the steady-state concentration of H_2O_2, $\overline{r_{H_2O_2}}$ denotes the average radiolytic production rate

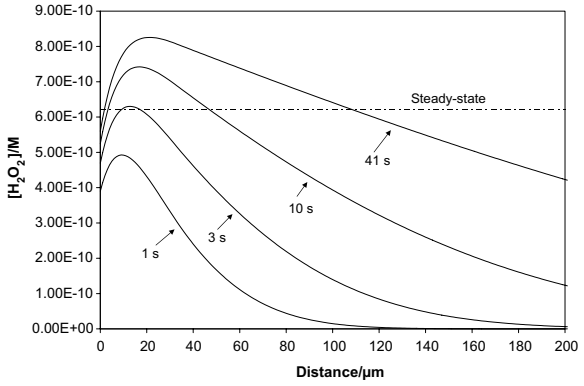

Fig. 1. H_2O_2 concentration profiles at 1, 3, 10 and 41 s for 100 years old spent fuel and $k = 7.33 \times 10^{-5}$ m s^{-1}.

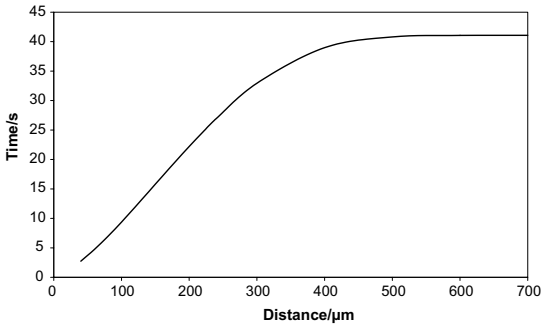

Fig. 2. Time to reach 90% of the steady-state surface concentration of H_2O_2 plotted against total distance used in the simulation.

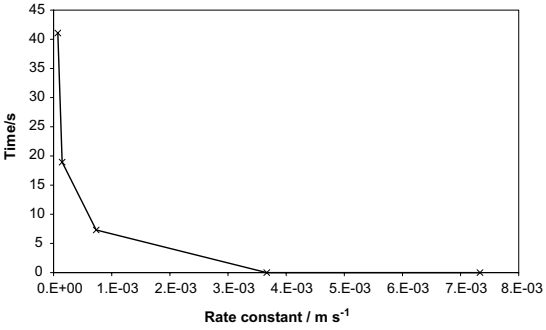

Fig. 3. Distance independent time to reach 90% of the steady-state surface concentration as a function of rate constant for H_2O_2 consumption.

for H_2O_2, δ_{max} is the maximum range for α-particles in water and k_{ox} is the rate constant used for the surface reaction. The steady-state expression is based on production and consumption of H_2O_2 per m^2 fuel surface.

As can be seen, the surface concentration fairly rapidly approaches the steady-state concentration. Consequently, the concentration gradient driving the diffusion of H_2O_2 from the surface into the bulk rapidly decreases and the surface reaction becomes the predominant pathway for H_2O_2 consumption. Since steady-state is approached asymptotically, the system will never reach a true steady-state. For this reason we have calculated the time required in order to reach a surface concentration corresponding to 90% of the steady-state concentration. After this point, the use of the steady-state concentration in simulating spent nuclear fuel dissolution will be less than 10%. In Table 1, the time to reach 90% of the steady-state surface concentration for different volumes (distances) and surface reaction rate constants are given. For the lowest rate constants the time to reach 90% of the steady-state concentration has only been calculated for short distances. The reason for this simply that the computation time becomes too long for longer distances.

As can be seen, the time to reach the predefined surface concentration increases with increasing volume (distance) and decreasing rate constant (increasing steady-state concentration). This is also illustrated in Figs. 2 and 3.

It is interesting to note that the time to reach 90% of the steady-state surface concentration appears to have a maximum value and, at a certain distance, becomes independent of the total distance. The distance at which the time to reach 90% of the steady-state concentration becomes independent of distance decreases with increasing rate constant. For the lowest rate constant (reflecting pure UO_2 reactivity) the distance at which the maximum time is reached cannot be calculated directly. However, on the basis of the results for some of the higher rate constants (the ratio between t(max) and t(40 μm) as well as the distance are inversely proportional to the rate constant) we estimate the maximum time to 187 days and the distance at which the time to reach 90% of the steady-state concentration becomes independent of the distance to 4 dm. Indeed, 187 days is significantly more than seconds or minutes but it can still be regarded as a fairly short time with

Table 1
Time to reach 90% of the steady-state surface concentration for different rate constants and distances

k (m s^{-1})	Time (s)						
	40 μm	60 μm	100 μm	200 μm	500 μm	1000 μm	2000 μm
7.33×10^{-8}	1546	2319	nd	nd	nd	nd	nd
7.33×10^{-7}	156	234	393	798	nd	nd	nd
7.33×10^{-6}	17	26	45	101	315	745	1510
7.33×10^{-5}	2.7	4.7	9.4	22.2	40.8	41.1	41.1
1.47×10^{-4}	2.0	3.5	6.9	14.8	18.9	18.9	18.9
7.33×10^{-4}	1.3	2.4	4.5	7.2	7.3	7.3	7.3

respect to the time frame for spent fuel dissolution. The above observations and the concentration profiles given in Fig. 1 illustrate a problem which can be encountered when analyzing data from spent fuel leaching experiments. It is obvious that bulk concentrations of H_2O_2 do not necessarily reflect the UO_2 dissolution rates since they can deviate significantly from the surface concentration. The fact that, for large enough distances, 90% of the steady-state concentration is reached within a maximum time independent of the total volume indicates that the actual geometry is of minor importance for the rate of spent fuel dissolution.

As the geometrical dose rate distribution is determined by the age of the spent nuclear fuel, it is important to study the effect of dose rate distribution on the time needed for reaching 90% of the steady-state concentration. The steady-state concentration is given by Eq. (4) and, as can be seen, the steady-state concentration is directly proportional to the average dose rate. Hence, a lower dose rate corresponds to a lower steady-state concentration. Simulations also show that the time needed for reaching 90% of the steady-state concentration is completely independent of the dose rate.

Thus, the only factors affecting the time needed for reaching steady-state is the rate constant for the surface reaction and, to a certain limit, the volume of the system.

Indeed, the above treatment of the system is simplified and in practice homogeneous reactions with species dissolved in the water will also affect the steady-state concentration of H_2O_2 in the system. One of the most important reactions is the reaction between H_2O_2 and Fe^{2+} (originating from the canister material) which, if present, will reduce the steady-state concentration as well as the time for reaching steady-state further.

From the results presented above it is clear that surface concentrations corresponding to 90% of the steady-state concentration will be reached within negligible time compared to the times of interest when simulating spent fuel dissolution under deep repository conditions. Consequently, simulation of spent fuel dissolution can be considerably simplified by using the steady-state approach. The inherent error imposed by using this approach is less than 10%. The procedure presented in this paper enables estimation of the maximum dissolution rate in a spent nuclear fuel repository.

Table 2
Calculated maximum rates of spent fuel dissolution

Fuel age (years)	r_{max} (mol m^{-2} s^{-1})
100	3.65×10^{-10}
1000	8.64×10^{-11}
10 000	1.65×10^{-11}
100 000	1.56×10^{-12}

Maximum dissolution rates based on the reactivity of pure UO_2 for spent fuel of ages 100–100 000 years are presented in Table 2.

It should be emphasized that the rate of radiation-induced dissolution of spent nuclear fuel can under no circumstances exceed these values. The presence of ε-particles and solutes reacting with H_2O_2 will reduce the rates significantly.

Acknowledgements

The Swedish Nuclear Fuel and Waste Management Company (SKB) and the Swedish Nuclear Power Inspectorate (SKI) are gratefully acknowledged for financial support.

References

[1] D.W. Shoesmith, J. Nucl. Mater. 282 (2000) 1.
[2] R.L. Segall, R.S.C. Smart, P.S. Turner, in: L.-C. Dufour (Ed.), Surface and Near-Surface Chemistry of Oxide Materials, Elsevier Science Publishers B.V., Amsterdam, 1988, p. 527.
[3] J.W.T. Spinks, R.J. Woods, An Introduction to Radiation Chemistry, John Wiley, New York, 1964.
[4] J.A.T. Smellie, M. Laaksoharju, P. Wikberg, J. Hydrol. 172 (1995) 147.
[5] P. Wardman, J. Phys. Chem. Ref. Data 18 (1989) 1637.
[6] R.E. Huie, C.L. Clifton, P. Neta, Radiat. Phys. Chem. 38 (1991) 477.
[7] I. Grenthe, F. Diego, F. Salvatore, G. Riccio, J. Chem. Soc. Dalton Trans. 11 (1984) 2439.
[8] E. Ekeroth, M. Jonsson, J. Nucl. Mater. 322 (2003) 242.
[9] M.M. Hossain, E. Ekeroth, M. Jonsson, J. Nucl. Mater. 358 (2006) 202.
[10] E. Ekeroth, O. Roth, M. Jonsson, J. Nucl. Mater. 355 (2006) 38.
[11] F. Nielsen, M. Jonsson, J. Nucl. Mater. 359 (2006) 1.
[12] M.B. Carver, D.V. Hanley, K.R. Chaplin, MAKSIMA-CHEMIST – A Program for Mass Action Kinetics Simulation by Automatic Chemical Equation Manipulation and Integration using Stiff Techniques, Atomic Energy of Canada Limited – Chalk River Nuclear Laboratories, Ontario, 1979.